Journal of Applied Geophysics 248 (2026) 106167

Contents lists available at ScienceDirect

Journal of Applied Geophysics

journal homepage: www.elsevier.com/locate/jappgeo

Seismic-attribute optimization for improving reservoir prediction integrating the spectral decomposition and automated machine learning

Keyu Ren [a,b], Wei Li [a,b], Lun Zhao [c], Wurong Wang [a,b], Jincai Wang [c], Han Wang [a,b], Yi Li [c], Linbo Qu [a,b], Dali Yue [a,b,*]

[a] State Key Laboratory of Petroleum Resources and Prospecting, China University of Petroleum, Beijing 102249, China
[b] College of Geosciences, China University of Petroleum, Beijing 102249, China
[c] PetroChina Research Institute of Petroleum Exploration & Development, Beijing 100083, China

ARTICLE INFO

Keywords:
Automated machine learning
Reservoir characterization
Seismic attribute fusion
Spectral decomposition

ABSTRACT

Seismic attribute analysis has served as a critical tool for geologists to uncover the geological characteristics of subsurface reservoirs. However, the geological information conveyed by seismic attributes of various types and frequencies exhibits significant diversity, due to complex nonlinear relationships between seismic attributes and sand thickness. Consequently, fully exploiting information embedded in seismic data and improving the seismic resolution for thin sand bodies has remained a key challenge in reservoir characterization. To address this challenge, we propose a novel intelligent approach to fuse multiple spectral-decomposed seismic attributes using an automated machine learning framework. This framework automates the training and integration of diverse algorithmic models without manual intervention, thereby improving both efficiency and predictive accuracy. By fusing seismic attributes across different frequencies and types, it significantly improves the resolution of reservoir prediction. This method was applied to the Zhetybay oilfield in Kazakhstan, significantly reducing uncertainty and improving the resolution of sandstone prediction. The predictions achieved a coefficient of determination of 0.878 (test dataset R^2). The proposed method provides a robust and efficient solution for quantitative sand prediction, which helps optimize well placement and reduce drilling risks in hydrocarbon exploration.

1. Introduction

Seismic data serves as a critical tool for accurately capturing underground geological information and plays an indispensable role in all phases of oil and gas exploration and development (Lin et al., 2024; Liu et al., 2018; Posamentier et al., 2022). Seismic attributes, as one of the primary methods for interpreting seismic data, have found extensive application in structural and stratigraphic interpretation, hydrocarbon detection, and reservoir prediction (Bashir et al., 2025; Chopra and Marfurt, 2005; Hampson et al., 2001; Posamentier et al., 2022; Yue et al., 2022). Through the extraction and analysis of relevant seismic attributes from seismic data, it is possible to characterize the distribution of geological bodies (especially channels and bars) and predict the scale of sand bodies along with their rock physical parameters (Hosseinyar et al., 2019; Yao et al., 2023; Zeng et al., 2001). This information is essential for comprehending underground geological conditions, formulating well-founded exploration and development strategies, and optimizing oilfield production processes.

Currently, numerous seismic attributes have been developed, each exhibiting different sensitivity to specific geological features, such as faults, sedimentary cycles and lithologies (Chopra and Marfurt, 2005; Koson et al., 2014; Li et al., 2020; Zhang et al., 2014). However, extensive evidence indicates that relying solely on seismic attributes for sandstone prediction entails significant uncertainties. This is due to the fact that the relationship between seismic attributes and sand thickness is influenced by multiple geological factors, resulting in a complex and nonlinear relationship (Li et al., 2023; Zeng, 2017). For instance, Seismic reflections from the top and bottom interfaces of a thin bed, such as a sandstone layer encased in mudstone, interfere with one another. This interference becomes maximally constructive when the bed thickness approaches the tuning thickness, which is approximately one-quarter of the dominant seismic wavelength ($\lambda/4$). This phenomenon, known as seismic tuning, generates a composite reflection amplitude that is significantly larger than that from either individual interface.

* Corresponding author at: State Key Laboratory of Petroleum Resources and Prospecting, China University of Petroleum, Beijing 102249, China.
E-mail address: yuedali@cup.edu.cn (D. Yue).

https://doi.org/10.1016/j.jappgeo.2026.106167
Received 23 November 2025; Received in revised form 16 January 2026; Accepted 13 February 2026
Available online 16 February 2026

Consequently, the tuning effect can distort the seismic response, leading to unrealistically high amplitudes for thin beds at or near the λ/4 thickness, which may not be representative of the bed's actual thickness (Bakke et al., 2013; Widess, 1973; Yue et al., 2019; Zeng and Backus, 2005). According to the tuning curves between sand thickness and amplitude, low-frequency amplitude attributes are more sensitive to thick sand bodies, while high-frequency amplitude attributes are more sensitive to relatively thin beds (Li et al., 2019). Therefore, integrating seismic attributes across different frequencies can remarkably enhance the resolution of reservoirs characterization (Li et al., 2025; Li et al., 2019; Yue et al., 2025; Yue et al., 2019; Zeng, 2017).

There are several methods for seismic multi-attribute fusion, which can be broadly categorized into color blending model, linear model fusion, and nonlinear model fusion (Yue et al., 2022). Color blending model enhances the image of geological phenomena by blending multiple attributes using a color model, such as the red-green-blue (RGB) model, without requiring well participation. This method has limitations on the number of fused attributes (Guo et al., 2008; McArdle and Ackers, 2012; Zeng, 2017). Linear model fusion involves combining multiple attributes through a linear algorithm or model after dimensionality reduction. This method is relatively simple but struggles to capture complex relationships, and may not be suitable for areas with dense well spacing (Al-Mudhafar, 2015; Hampson et al., 2001). In the context of nonlinear model fusion, machine learning algorithms have been widely employed to perform regression fitting on multiple seismic attributes for reservoir characterization. For instance, Support Vector Machine (SVM) has been among the first algorithms applied in this field, leveraging its advantage in small-sample scenarios to predict sand body thickness from integrated seismic attributes (Li et al., 2019; Na'imi et al., 2014). The k-Nearest Neighbors (KNN) algorithm has also been adopted to construct regression models for sand body thickness prediction (Ballinas et al., 2023). In addition, Gradient Boosting Decision Trees (GBDT) and Artificial Neural Networks (ANN) have also found extensive applications in this domain (Abdulaziz et al., 2019; Iturrarán-Viveros and Parra, 2014; Jia et al., 2023).

The distribution of sand bodies is controlled by the complex interactions among sedimentary systems, tectonic deformation, and diagenesis, resulting in significant heterogeneity both regionally and between stratigraphic layers (Pang et al., 2024; Xu et al., 2025). This complexity prevents any single machine learning algorithm from delivering stable performance in diverse geological contexts, necessitating repeated model selection and parameter tuning for different reservoirs and layers—an effort-intensive and time-consuming process. Ensemble learning has been increasingly adopted in reservoir characterization, combining multiple base learners to improve prediction stability and generalization (Ali et al., 2023; Anifowose et al., 2017). However, constructing effective ensemble models, specifically regarding the choice of learners, weighting strategies, and hyperparameter optimization, necessitates profound algorithmic expertise. This requirement creates a technical barrier for operators who may lack specialized training. Moreover, the conventional manual tuning through exhaustive trials is inefficient, irreproducible, and often require excessive time investments ranging from days to months. As geological conditions or data characteristics change, even well-tuned ensemble configurations may degrade over time if not adapted to new data. Thus, a key challenge in intelligent reservoir characterization is to design ensemble frameworks capable of self-adaptive evolution, complementing expert knowledge with systematic robustness and improving the generality of predictions across diverse operational scenarios.

Automated Machine Learning (AutoML) has emerged as a promising solution to these challenges. AutoML streamlines the machine learning workflow by automating critical tasks, including feature engineering, model selection, hyperparameter optimization, model ensembling, interpretability analysis, and multi-metric performance evaluation (He et al., 2021; Quaranta et al., 2025; Salehin et al., 2024; Shen et al., 2018; Zöller and Huber, 2021). This approach streamlines deployment, allowing for effective implementation that prioritizes usability and reduces procedural complexity. At present, AutoML has yet to be applied to fuse seismic attributes, but it offers a novel prospective to integrate them more efficiently and accurately for sand body thickness prediction.

In this study, we propose an AutoML-based intelligent approach for fusing spectral-decomposed attributes that automatically train, integrates multiple models, and optimizes hyperparameters—requiring no extra coding or manual adjustment. In the Zhetybay Oilfield, this framework significantly improves the accuracy and robustness of reservoir sand body prediction.

2. Geological setting

The Zhetybay oilfield is situated on the northern margin of the Mangyshlak Basin in southwestern Kazakhstan and is located 80 km southeast of Aktau City (Fig. 1A). It is a large and gentle long-axis anticlinal structure with a nearly southeast-northwest trend (Ni et al., 2022). The study area is located in the eastern part of the Zhetybay oilfield and covers an area of approximately 60km^2 (Fig. 1A).

The stratigraphic development strata of the Zhetybay Oilfield, arranged in ascending order, includes the Carboniferous, Permian, Jurassic, Cretaceous, Paleogene, Neogene, and Quaternary (Fig. 1B). The Middle Jurassic fluvial-delta sandstone reservoirs represent the principal hydrocarbon-producing formation within this oilfield (Kiritchkova and Nosova, 2014). The lithology is primarily composed of argillaceous fine-grained sandstone and siltstone, with intercalated dark-gray to gray compacted argillaceous beds occurring recurrently (Cherskiy et al., 1984). The stratigraphic interval of interest is part of the lower Bathonian Formation (Jurassic, Mesozoic) (Fig. 1C), which is interpreted as a delta front deposited (Ni et al., 2022). This target formation is Zone 3, ranging in thickness from 12 m to 30 m (Fig. 1C). The depth of the formation ranges from 1950 m to 2050 m. The reservoirs have medium porosities (16.5–19.1%) and medium permeabilities (50–224 mD).

3. Dataset

The dataset of the study area comprises 621 wells and a 3D seismic volume. Most wells are equipped with comprehensive logging curves and lithological interpretations, including spontaneous potential (SP), gamma ray (GR), deep laterolog (LLD), and shallow laterolog (LLS). Lithological interpretation is conventionally performed by analyzing the characteristic responses recorded by well logging. A statistical analysis of interpreted sandstone thicknesses from our dataset reveals a primary concentration within the 4–25 m range. More specifically, sandstone with thicknesses less than 10 m constitute approximately 19.4% of the total, while those ranging from 10 to 16 m represent the largest proportion at 58.9%. Sandstone exceeding 16 m in thickness accounts for the remaining 21.7% (Fig. 2A). Lithological interpretation in well provides a target variable for model training, making it possible to transform seismic attributes into lithology. Furthermore, the frequency distribution of sandstone thickness offers guidance for spectral decomposition. The 3D seismic volume is post-stack processed to achieve near-zero phase, with a dominant frequency of 50 Hz and an effective bandwidth of 6–94 Hz (Fig. 2B). The vertical sampling interval is 2 ms, while both the inline and crossline intervals are 15 m. Based on acoustic wireline log statistics, the P-wave velocity within the study formation ranges from 3000 m/s to 3500 m/s (average is 3252 m/s). Generally, well data and seismic data exhibit different resolutions. Well data, such as logging curves and cores, possess centimeter-level vertical resolution, whereas spatial interpolation derived from 1D well data introduces significant uncertainty. In contrast, seismic data have lower vertical resolution (λ/4 close to 16 m) but higher lateral resolution, compared to 1-D well data.

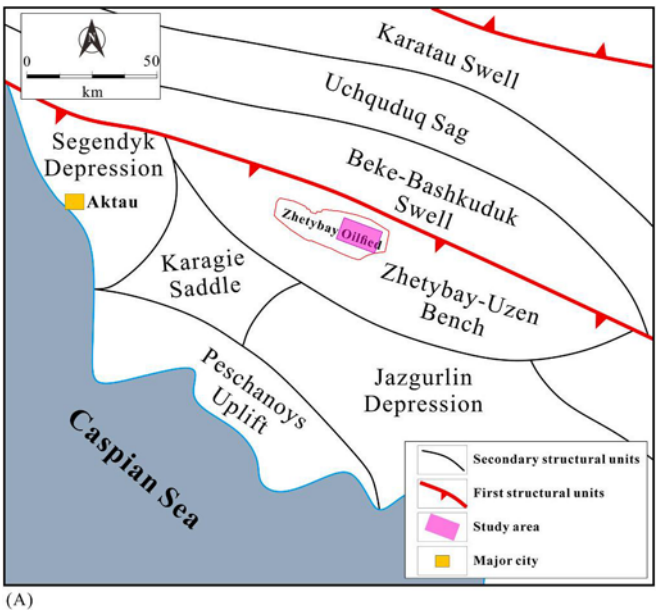

Fig. 1. A) Tectonic framework of the northern margin of the Mangyshlak Basin (modified after Ni et al., 2022). The red polygon highlights the Zhetybay oilfield. B). Stratigraphic chart of the Mangyshlak Basin with basin evolution phases (modified after Kozhagulova et al., 2023). C) Profile of Well 4840 in the lower Bathonian Formation of the Middle Jurassic, showing gamma ray (GR), acoustic (AC), and density (DEN) logs, along with the interpretation of lithology and sedimentary facies. (For interpretation of the references to color in this figure legend, the reader is referred to the web version of this article.)

4. Methodology

We develop an automated machine learning approach for fusing seismic attributes in quantitative reservoir characterization. The method integrates seismic spectral decomposition, attributes selection, and AutoML-based spectral-decomposed attributes fusion.

4.1. Integrated workflow of the proposed method

We utilized an automated machine learning (AutoML) approach for fusing seismic attributes to predict the thickness of sandstone. This consists of four workflow segments: decomposing the original seismic volume, selecting the appropriate seismic attributes, extracting the thickness of sandstone and the seismic attributes around wells to construct the dataset, and training the AutoML model to fuse the selected spectral-decomposed seismic attributes (Fig. 3).

Prior to the formal process, Synthetic seismograms were generated to tie the wells to seismic data in the time domain, matching the well tops with corresponding seismic horizons. First, the original seismic data volume undergoes spectral decomposition, and the spectral characteristics of the resulting frequency bands are analyzed (Fig. 3A). Second, we performed correlation analysis and unsupervised clustering to select the most representative seismic attributes and extracted the attributes from spectral-decomposed seismic volumes based on the selection results (Fig. 3B). Third, the thickness of sand bodies derived from well logs and the average seismic attribute values around well points (within a radius of 15 m) are extracted to construct the training dataset (Fig. 3C). Finally, the AutoML model is trained to integrate multiple spectral-decomposed seismic attributes, thereby enabling the quantitative prediction of reservoir properties (Fig. 3D).

4.2. Spectral decomposition via continuous wavelet transform

Seismic data volumes of various frequency bands contain distinct geological information. A thorough investigation into the relationship between seismic data of various frequency bands and reservoir characteristics significantly improves the resolution of reservoir prediction. Due to the influence of tuning effects on seismic response (Widess, 1973; Zeng, 2017), a nonlinear relationship exists between amplitude and frequency for reservoirs of varying thicknesses (Li et al., 2020). To further clarify the mechanism, a wedge forward model (max thickness 30 m) was convolved with Ricker wavelets to investigate the amplitude-thickness relationship (Fig. 4A). The tuning curves show that amplitude correlates positively with thickness below the tuning thickness ($\lambda/4$) but stabilizes for thicker beds. Low-frequency bands favor thick sand bodies, whereas high-frequency bands provide better resolution for thin beds. Therefore, relying on single-frequency seismic attributes for thickness prediction often results in ambiguity. For example, a normalized amplitude of 0.82 in the 75 Hz model corresponds to thicknesses of both 6 m (Point A) and 15 m (Point B). However, incorporating amplitudes from the 26 Hz (Point C) and 51 Hz (Point D) models resolves this non-uniqueness, identifying 15 m as the correct thickness. This confirms that multi-frequency integration significantly reduces uncertainty in thickness prediction.

Although various methods are available for seismic decomposition, continuous wavelet transform (CWT) has been established as a reliable, robust, and widely used approach (Shahsenov et al., 2022; Zhang et al., 2025). Therefore, this study employs CWT to decompose the original seismic volume into several spectral-decomposed seismic volumes of differing frequencies and bandwidths. The basic idea behind CWT is the wavelet implementation as a band-pass filter to the time series signal. Specifically, it is implemented through convolution of seismic traces $s(t)$ with scaled mother wavelets ψ (Sinha et al., 2005):

$$S(a,b) = \frac{1}{\sqrt{a}} \int_{-\infty}^{\infty} s(t) \psi^* \left(\frac{t-b}{a} \right) dt \tag{1}$$

where a denotes scale parameter (inversely proportional to frequency), b represents temporal translation, and $s(t)$ denotes the signal to be analyzed, $\psi^*(t)$ denotes the complex conjugate of the mother wavelet.

The Morlet wavelet, a widely adopted mother wavelet for CWT, has consistently demonstrated simplicity, computational efficiency, and high accuracy in a broad range of studies (Cai et al., 2024; Xue et al., 2014). Therefore, the CWT decomposition using the Morlet wavelet as

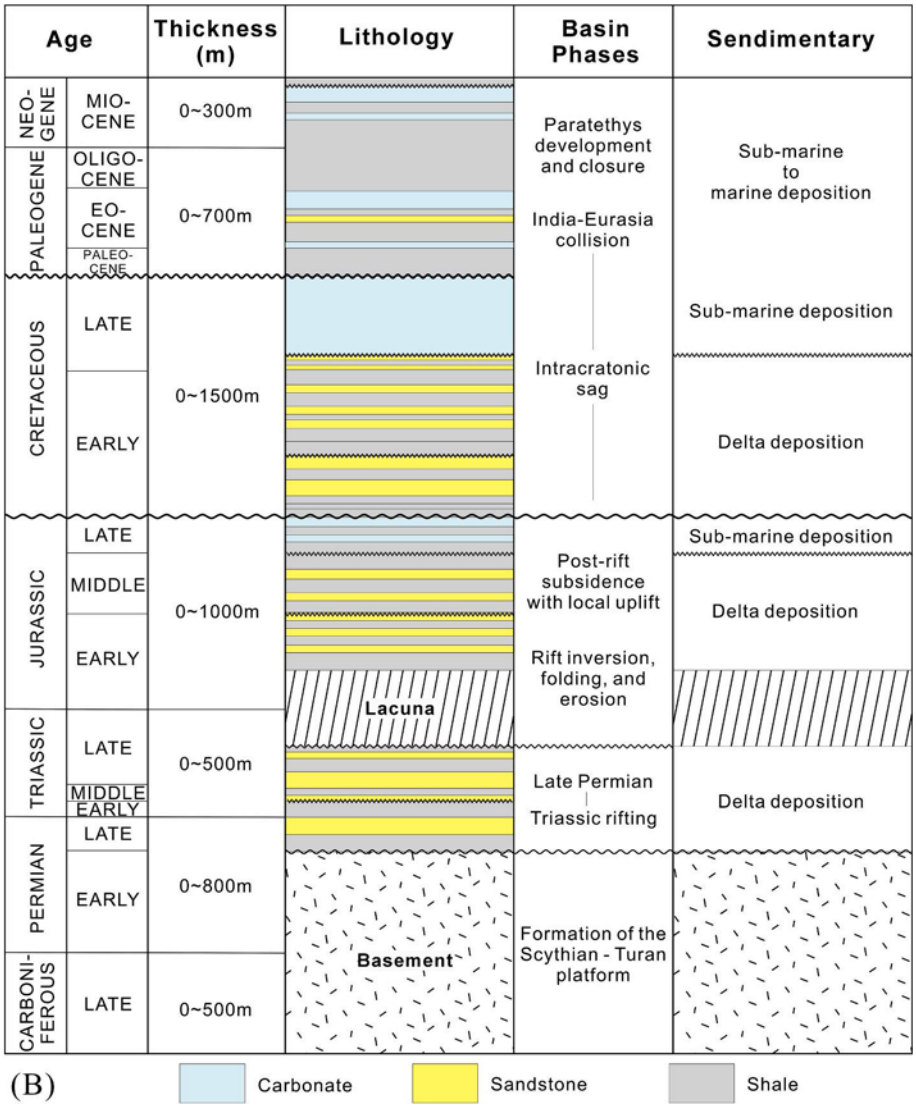

Fig. 1. (*continued*).

the mother wavelet was employed to decompose the original seismic data volume in this study. The selection of effective bandwidths, dominant frequencies, and the total number of spectral-decomposed seismic volumes is critical and should adhere to two primary principles. First, the chosen dominant frequencies must lie within the effective bandwidth of the original seismic data to ensure a high signal-to-noise ratio. Second, the number of spectral-decomposed seismic volumes should be limited to prevent redundancy in the seismic data. In practice, geologists may choose spectral-decomposed seismic volumes with suitable dominant frequencies based on specific research objectives. Following these guidelines, the original seismic volume in this study was decomposed into three distinct frequency bands: low-, middle-, and high-frequency spectral-decomposed seismic volumes (Fig. 4B).

In seismic spectral decomposition using the CWT, the Cone of Influence (COI) introduces systematic boundary effects that can directly compromise the reliability of decomposed attributes and the quality of subsequent imaging. There is no mathematically precise rule to determine the extent of the COI at each scale. However, since many of the wavelets used in continuous wavelet analysis decay exponentially in time, it is conventional to use the time constant 1/e to delineate the borders of the COI at each scale (Torrence and Compo, 1998). In this dataset, the target zone (1450–1550 ms) is centrally located within the full 0–3000 ms seismic record. This provides a safety margin of over 1400 ms from the data boundaries, which is far larger than the range of the COI. Therefore, the target zone lies entirely outside the region of boundary effects, ensuring the reliability and high quality of the spectral decomposition results.

4.3. *Automated machine learning framework*

Machine learning (ML) has become a cornerstone of modern technological and business innovation. However, traditional ML development processes demand extensive domain expertise and time-intensive iterations, posing substantial challenges for inexperienced teams or individuals. To mitigate these limitations, AutoML has emerged as a transformative solution, significantly lowering the technical barrier and enabling developers to deploy high-performance models with enhanced efficiency (He et al., 2021; Shen et al., 2018; Zöller and Huber, 2021). Among existing tools, AutoGluon, an open-source framework developed by the Amazon Web Services (AWS) team, stands out for its emphasis on user accessibility, computational efficiency, flexibility, and cross-modal compatibility (Erickson et al., 2020).

In this study, we proposed a novel AutoML-based intelligent fusion approach for spectral-decomposed attributes using the open-source AutoGluon framework. We optimized the AutoGluon framework to better apply to the specific needs of quantitative reservoir prediction and

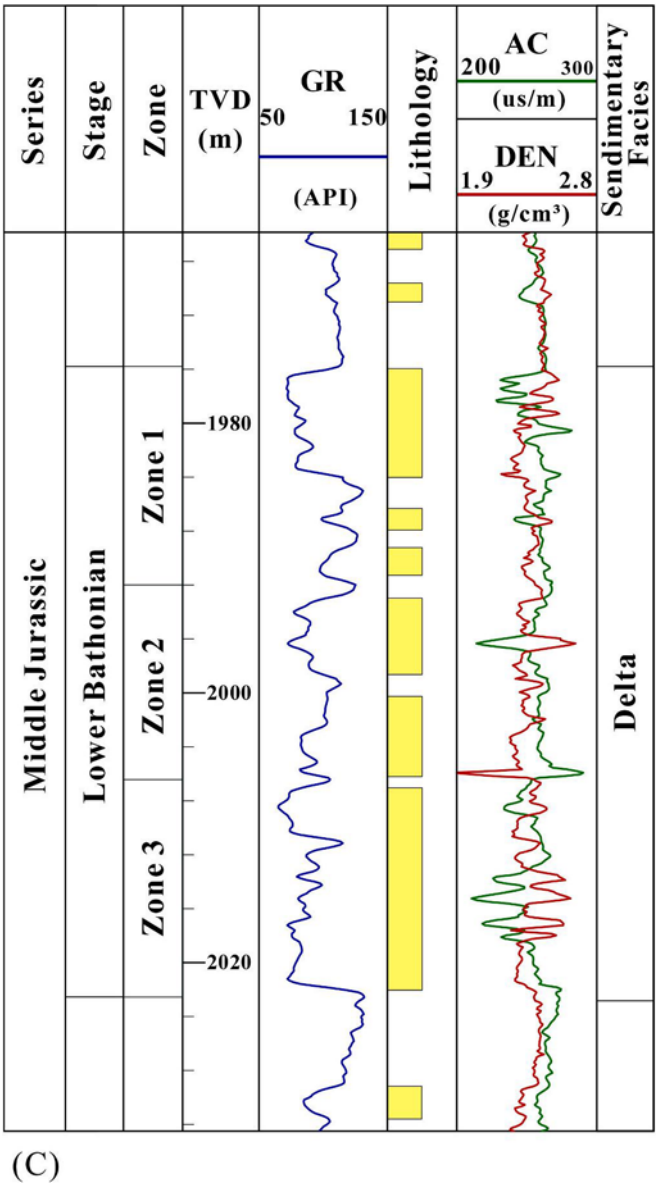

Fig. 1. (*continued*).

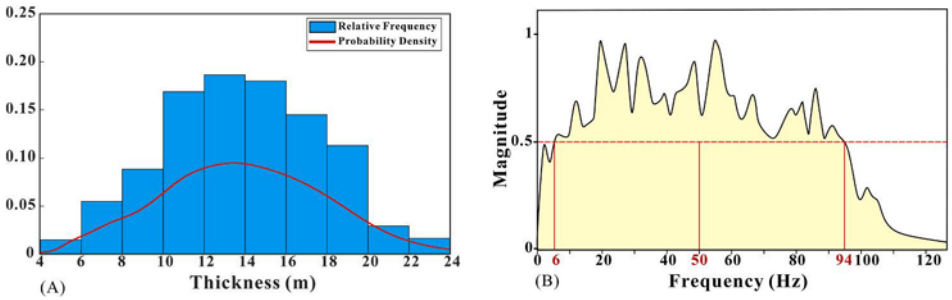

Fig. 2. Statistical characteristics of sandstone thickness distribution and normalized spectra of the original 3D seismic volumes of the Lower Bathonian Formation in the study area. A) Histogram of sandstone thickness derived from well-log interpretation, it is mainly concentrated in the 10–18 m interval, accounting for 79.4%. Blue indicates relative frequency, while the red curve denotes the probability density B) Original 3D seismic volume with a bandwidth of 6–94 Hz and a dominant frequency of 50 Hz. (For interpretation of the references to color in this figure legend, the reader is referred to the web version of this article.)

seismic attributes fusion. The approach enables end-to-end automation of model training and ensemble processes through three core components: data input and preprocessing (Fig. 5A), model training (Fig. 5B), and model evaluation (Fig. 5C).

The workflow begins with data preprocessing (Fig. 5A), input seismic attributes are preprocessed through data alignment, noise reduction,

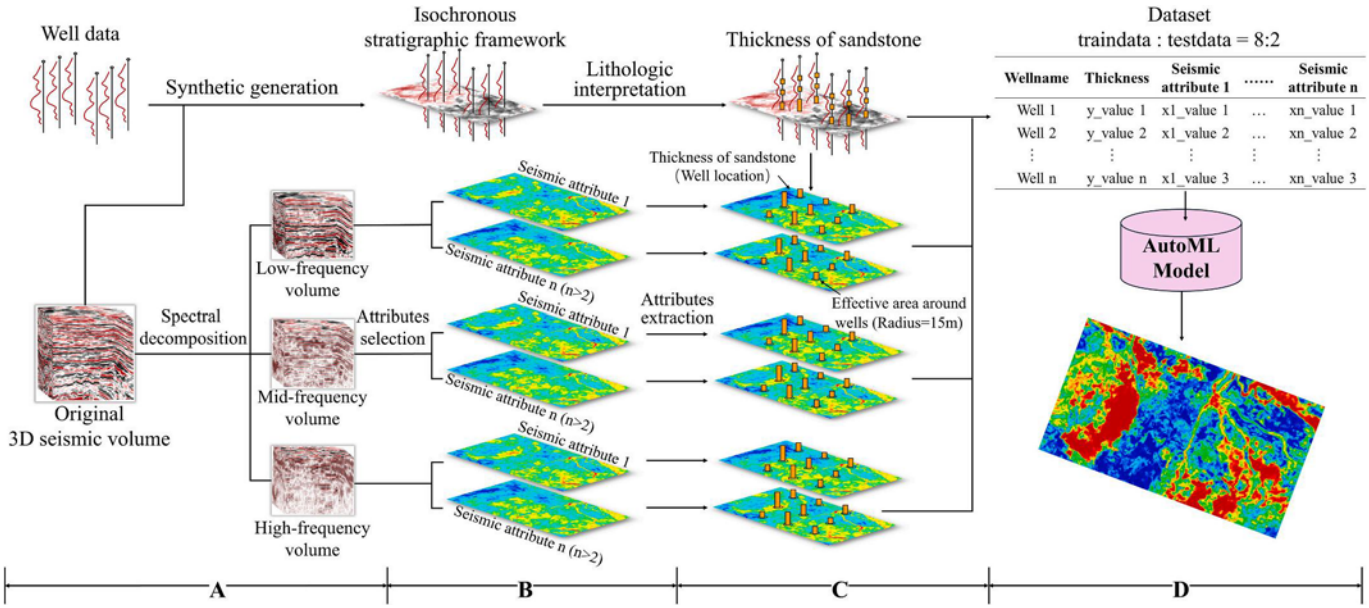

Fig. 3. The workflow diagram outlines the methodology of fusion of spectral-decomposed attributes using an AutoML model. A) Decomposing the original seismic volume. B) Selecting the appropriate seismic attributes. C) Extracting the thickness of sandstone and seismic attributes value around wells to construct the dataset. D) Training the AutoML model to fuse the selected spectral-decomposed seismic attributes.

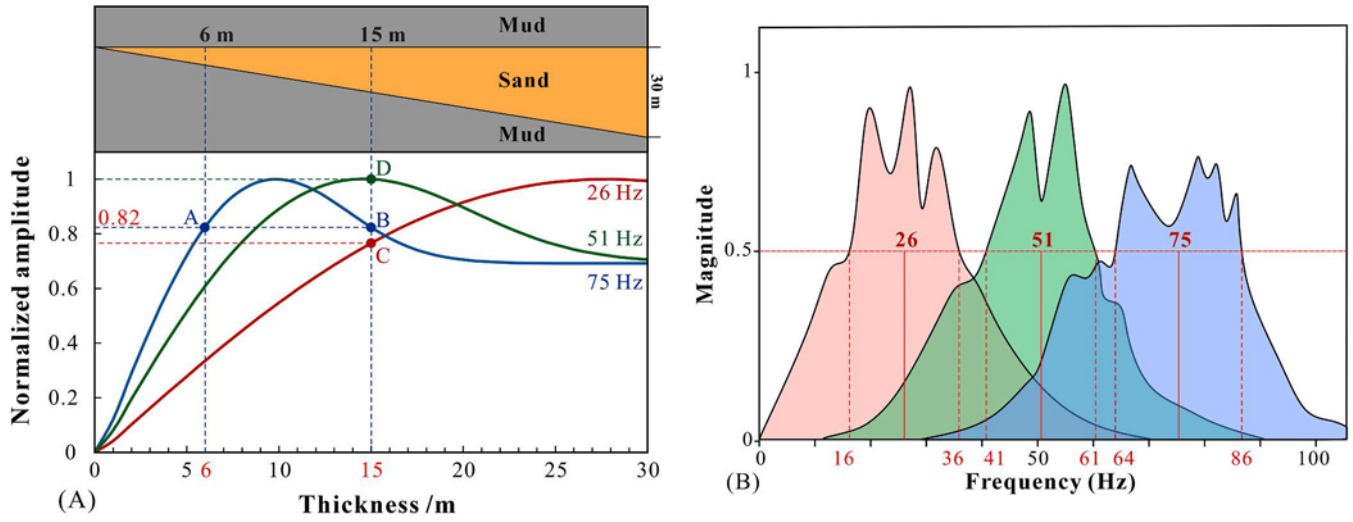

Fig. 4. A) Forward wedge model and tuning curves showing amplitude vs. thickness for different frequency Ricker wavelets. Model parameters were derived from the study area, the velocity and density of mudstone are 3337.1 m/s and 2.34 g/cm^3, velocity and density of sandstone are 3166.9 m/s and 2.36 g/cm^3 respectively. B) Parameters for the spectral decomposition volumes. The low-, middle-, and high-frequency spectral-decomposed seismic volumes have dominant frequencies of 26 Hz, 51 Hz, and 75 Hz, and bandwidths of 16–36 Hz, 41–61 Hz, and 64–86 Hz. These correspond to tuning thicknesses of 30 m (low), 15 m (mid), and 10 m (high), respectively.

and normalization (Normalized to dimensionless values in the [0,1] range). Before being partitioned into training and testing datasets (8:2), with the testing dataset serving as an independent blind dataset. For model training (Fig. 5B), the framework executes model training and ensemble, leveraging its automated pipelines. Model ensemble was achieved through a composite strategy involving multi-layer stacking with repeated k-fold bagging. The first layer integrates diverse base models, each optimized via auto hyperparameter optimization (Auto-HPO). Auto hyperparameter optimization employed Bayesian optimization, which efficiently explores the parameter space by leveraging prior knowledge and observed outcomes to identify near-optimal configurations with minimal evaluations. Predictions from these base models are concatenated and propagated to subsequent layers for iterative refinement. Crucially, higher-layer stackers incorporate both lower-layer predictions and the original input features, thereby retaining access to raw data patterns during training. The final layer employs an ensemble selection to compute weighted aggregations of stacker predictions. To further mitigate overfitting risks, the framework implements a repeated k-fold bagging mechanism: the framework iteratively applies k-fold bagging across n randomized partitions of the training dataset, averaging out-of-fold predictions over all repetitions. The parameter n is dynamically determined based on the estimated computational capacity within the allocated training duration.

After training completion, the trained meta-model is evaluated on both training and testing datasets (Fig. 5C), with its performance primarily assessed against key metrics such as the coefficient of determination (R^2) and the Mean Absolute Error (MAE). Should the result of output fail to satisfy predefined criteria (e.g., $R^2 > 0.8$ and MAE < 2),

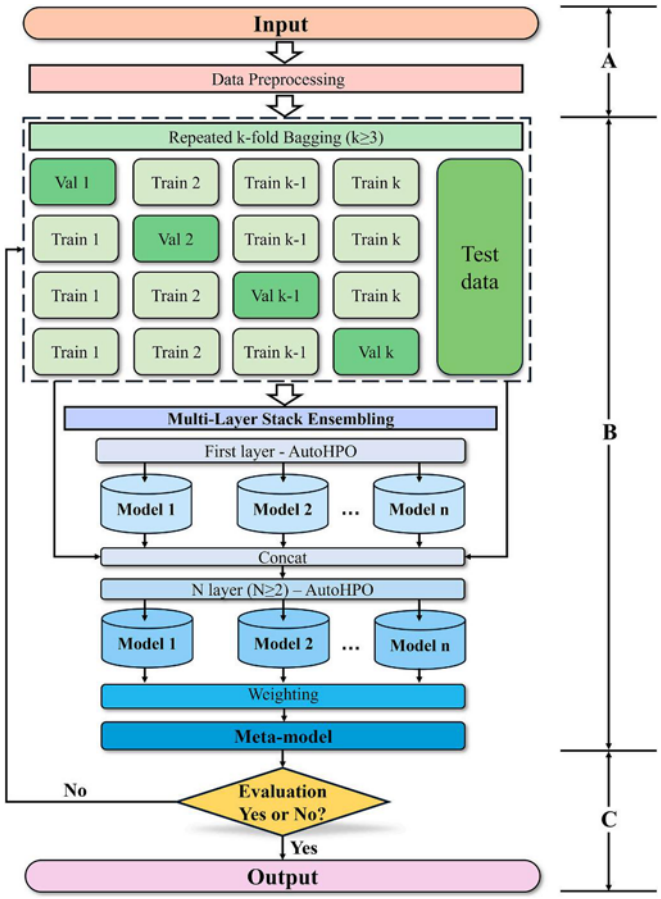

Fig. 5. Workflow of the proposed AutoML framework. Bold characters on the right indicate the sections referred to in the text. (A) Data input and preprocessing. (B) Model training and ensemble. The model is trained using a multi-layer stacking ensemble, where each base learner is optimized via Bayesian hyperparameter tuning and combined using repeated k-fold bagging to mitigate overfitting. (C) Model evaluation. The trained meta-model is evaluated on both cross-validation and testing datasets.

iterative adjustments to input data and algorithmic configurations are implemented until the model achieves the desired performance thresholds.

We developed a multi-layer ensemble prediction system based on the AutoGluon framework, incorporating a 3-layer stacked architecture with repeated 5-fold Bagging to mitigate overfitting. When selecting algorithm types, the following principles should be followed: selected algorithms should be well-established and maturely applied in seismic attribute analysis or reservoir characterization, and the algorithms should encompass diverse categories to address datasets with different statistical distributions. Therefore, we selected 8 representative algorithms spanning diverse categories (Table 1) (Bao et al., 2023; Haiyang et al., 2023; Liu et al., 2024; Tian et al., 2021). This diversified portfolio ensures comprehensive exploration of both conventional and emerging approaches in reservoir prediction tasks.

Table 1
The selected algorithms that demonstrate mature performance in reservoir characterization.

No.	Category	Algorithms
1	Bagging Learners	Random Forest (RF), Extra Randomized Trees (ERT)
2	Gradient Boosting	CatBoost (CAT), XGBoost (XGB), LightGBM (LGBM)
3	Instance-based	K-Nearest Neighbors (KNN)
4	Neural Network	NeuralNetTorch (NNT), NeuralNetFastAi (NNFAI)

5. Results

5.1. Original seismic attributes and spectral-decomposed seismic attributes

5.1.1. Dual-parameter seismic attributes optimization

To mitigate significant collinearity among redundant attributes, systematic attribute selection was conducted prior to multi-attribute integration. A dataset comprising 621 wells with comprehensive logging records was analyzed. Average seismic attribute values were calculated within a 15-m radius around each well location. The optimization process of seismic attributes adhered to two fundamental principles. First, attributes exhibiting a high correlation with sand thickness were prioritized to ensure a robust predictive relationship. Second, to prevent information redundancy, the selected attributes were required to maintain relative independence, thereby minimizing the effects of inter-attribute correlation and avoiding redundancy. Accordingly, a cross-correlation analysis between attributes and sand thickness was performed, and the nine attributes with the highest correlation were selected for further cluster analysis (Fig. 6A). These attributes were subsequently classified into four clusters using unsupervised K-means clustering (Fig. 6B). Within each cluster, attributes demonstrating stronger correlations with sand thickness were prioritized. Through this hierarchical selection process, the optimal sensitive attributes identified were Sweetness, Envelope, and RMS Amplitude.

5.1.2. Spectral decomposition of seismic volume

According to the statistical results, the target-layer sandstone thickness follows an approximately normal distribution and varies primarily between 4 and 25 m (Fig. 2A). We considered the thickness less than 10 m as thin beds, while those exceeding 16 m were defined as thick beds. The original seismic data volume, with a bandwidth of 6–94 Hz and a dominant frequency of 50 Hz (Fig. 2B), was subjected to spectral decomposition using the method described in Section 4.2. Based on the Morlet wavelet, we utilized CWT to decompose the original seismic volume into multiple spectral-decomposed seismic volumes with varied dominant frequencies and bandwidths. Wedge modeling (Fig. 4A) confirms that the spectral volumes target specific thickness ranges: the high-frequency (75 Hz), medium-frequency (51 Hz), and low-frequency (26 Hz) volumes exhibit linear, positive responses across 4–10 m, 10–16 m, and 16–25 m intervals, respectively. Consequently, three spectral-decomposed seismic volumes (Fig. 4B) are capable of effectively resolving their corresponding thickness intervals, ensuring robust detection capabilities for the entire range of sandstone thicknesses.

5.1.3. Seismic attributes characterization

Following the result of attributes optimization, we extracted 3 seismic attributes (RMS amplitude, envelope, and sweetness) from original and spectral-decomposed seismic volumes. Among these, the sweetness attribute exhibited the maximum Correlation coefficient (0.450) with sand thickness (Fig. 6A). The sweetness attribute exhibits superior correlation due to its mathematical formulation, defined as the instantaneous amplitude divided by the square root of the instantaneous frequency (Hart, 2008). This formulation effectively amplifies the high-amplitude, low-frequency signature typical of sandstone beds while simultaneously suppressing the contrasting seismic response of the surrounding mudstone. Therefore, this attribute was selected as a representative example to analyze the imaging characteristics of various spectral-decomposed seismic attributes.

Frequency-dependent variations in the sweetness attribute revealed that increasing dominant frequencies correlate with high sweetness values corresponding to thin sand bodies. In the original sweetness attribute map, high-value areas partially reflect the distribution of sand bodies, while the channel boundaries are generally recognized in the eastern study area (Fig. 7A). The low-frequency sweetness map displays

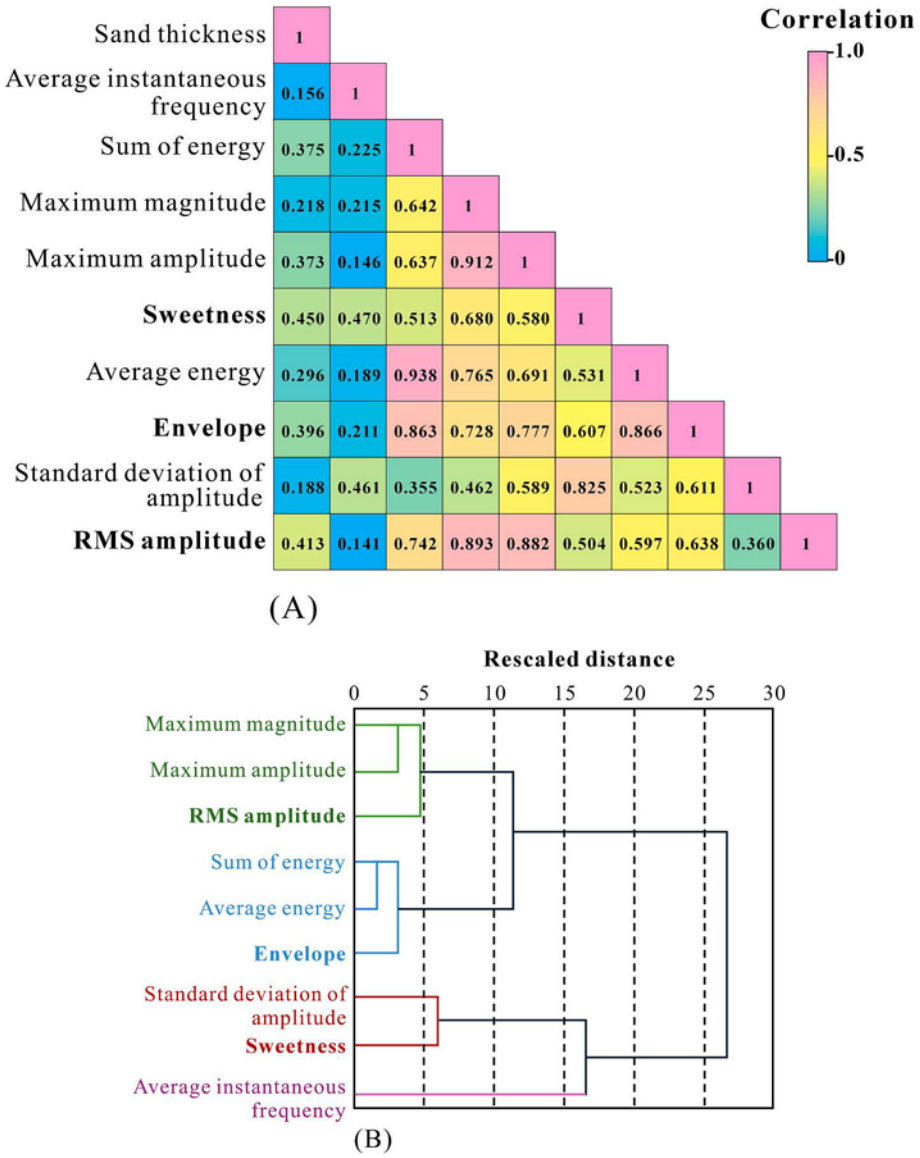

Fig. 6. Seismic attributes correlation analysis and unsupervised clustering. A) Heatmap of the correlation between the nine seismic attributes and sand thickness from well logs. B) Dendrogram of the selected seismic attributes with unsupervised cluster analysis. Green lines: cluster 1; blue lines: cluster 2; red lines: cluster 3; purple lines: cluster 4. (For interpretation of the references to color in this figure legend, the reader is referred to the web version of this article.)

a lobate morphology in the western region (Fig. 7B), with values significantly higher than those observed in equivalent location of the high-frequency sweetness map. Conversely, the high-frequency sweetness map demonstrates enhanced continuity and clarity in channel boundary delineation within the eastern region (Fig. 7D). Well-log interpretations confirm that the western lobate feature (highlighted in red) corresponds to sand bodies exceeding 20 m in thickness, whereas the eastern channel-bar complexes comprise thinner sands (<14 m). These observations suggest that high-frequency seismic attributes exhibit superior resolution in delineating boundaries and imaging thin sand bodies, while low-frequency attributes are more effective in estimating thicknesses of thicker sand bodies.

5.2. *Fused spectral-decomposed seismic attributes and prediction of sand bodies*

For each of the 621 wells, the mean values of spectral-decomposed seismic attributes within a 15 m radius were extracted and designated as feature variables, whereas the sandstone thickness from wells served as the target variable. These data were compiled to establish the complete dataset, which was then randomly partitioned into training and testing subsets at an 8:2 ratio. The training subset was exclusively used for model training, while the testing subset (blind dataset) was reserved for evaluating the predictive performance of the model. Model performance was assessed using four evaluation metrics: Pearson correlation coefficient (R), coefficient of determination (R^2), root mean squared error (RMSE) and mean absolute error (MAE). These evaluation metrics are widely acknowledged as standard metrics for evaluating the performance of regression prediction models. Specifically, R and R^2 primarily measure the goodness of fitting (with values closer to 1 indicating better fitting) (Krause et al., 2005). MAE evaluates the accuracy of the prediction results, where smaller values signify closer alignment with observed values. RMSE measures the difference or error between the predicted with observed values, with lower values reflecting superior model performance in terms of stability and accuracy (Liu et al., 2024; Nash and Sutcliffe, 1970). To ensure statistical reliability, 10 independent trials were conducted, with all regression results recorded in Table 2.

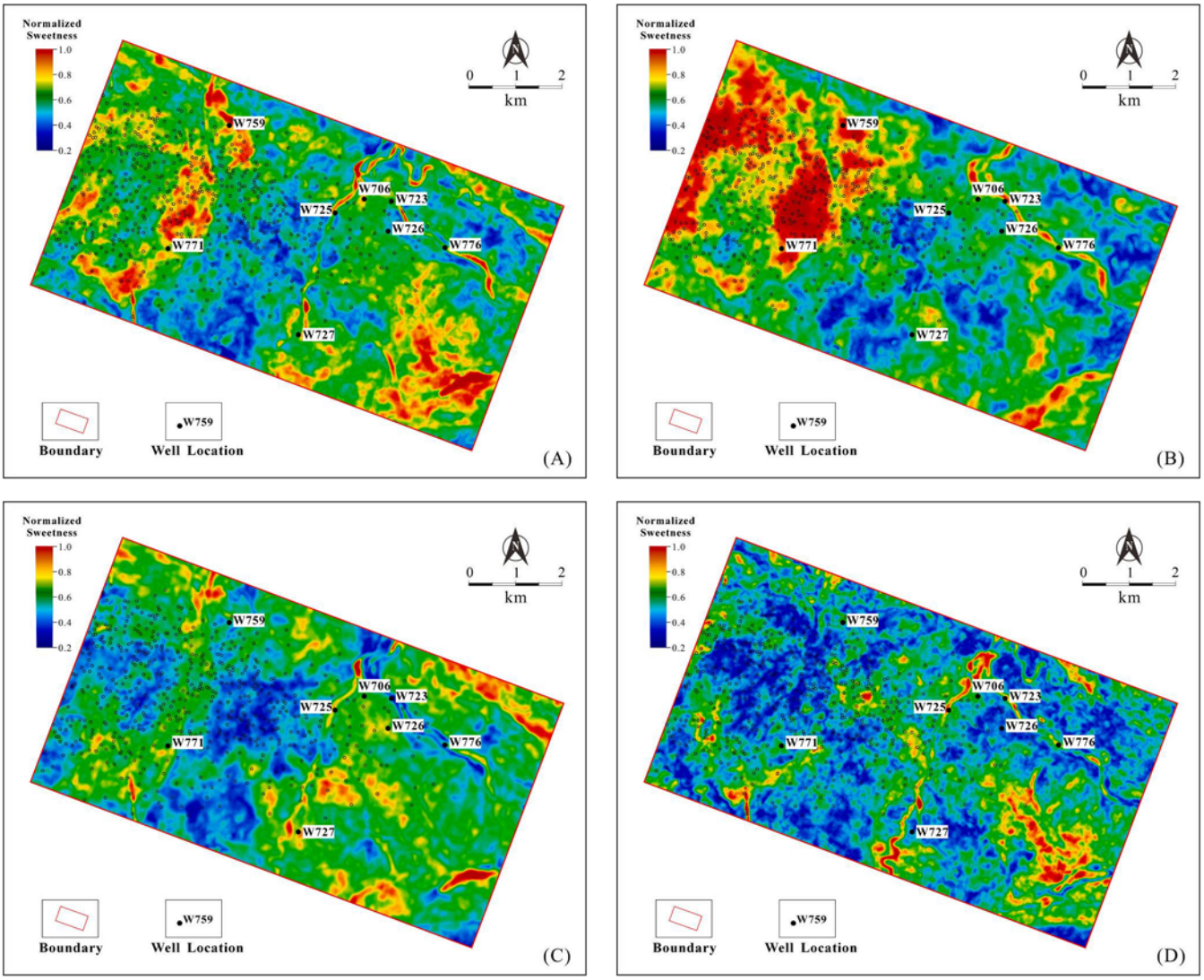

Fig. 7. Original seismic Sweetness attribute and spectral-decomposed seismic Sweetness attributes. A) Original seismic Sweetness attribute. Extracted from the original seismic data volume, this attribute exhibits limited clarity in distribution of sandstone. B) Low-frequency seismic Sweetness attribute. Extracted from the low-frequency seismic data volume, this attribute shows broadly distributed high-value regions. C) Mid-frequency seismic Sweetness attribute. Extracted from the mid-frequency seismic data volume, this attribute displays reduced high-value regions. D) High-frequency seismic Sweetness attribute. Extracted from the high-frequency seismic data volume, this attribute enables partial identification of sandstone distribution boundaries. The sandstone thickness from well logs (ST) is shown in the white box.

Single-model analysis revealed substantial performance disparities (Table 2). The KNN algorithm exhibited the weakest performance (R = 0.730), with the highest RMSE (2.471) and MAE (2.051). In contrast, neural network models demonstrated superiority: NNT (R = 0.873, MAE = 1.799) and NNFAI (R = 0.870, MAE = 1.808) ranked as the top two performers, showing statistically significant improvements in R over the third-placed CAT (0.868) model. The inferior performance of KNN aligns with its inherent sensitivity to data noise and feature scaling (Halder et al., 2024), exacerbated by the significant magnitude differences (10^3 orders) between seismic attributes such as RMS amplitude and sweetness. Notably, all single models achieved MAE below 2.5, with gradient-boosting algorithms also exhibiting good numerical stability.

The AutoGluon-optimized Meta-Model demonstrated substantial performance enhancements (Table 2), achieving a R of 0.926 (6.1% increase) and R^2 of 0.832 (13.4% increase) compared to the best individual model (NNT), while concurrently reducing the RMSE from 2.246 to 1.898 (a decrease of 15.5%), and the MAE from 1.799 to 1.503 (a decrease of 16.5%), respectively. Compared with the KNN model, which demonstrated the poorest performance, the Meta-Model achieved a 66.4% increase in R^2 and a 26.7% decrease in MAE. Consequently, the framework was employed to fuse low-, mid-, and high-frequency seismic attributes, and the fused result directly represented the thickness of the sand bodies in the target layer. The reproducibility analysis revealed that the results of 10 experiments were very similar (Fig. 9). Therefore, we merely showed the result of the 9th trial (Fig. 8), which performed the best. The boundaries of the sand bodies were distinct, and the sand thicknesses were visualized and quantified (Fig. 8). The prediction results on the independent test dataset indicated that the correlation coefficient between the prediction and the actual sand thickness from wells was 0.937, confirming its practical utility in complex stratigraphic interpretation.

6. Discussion

6.1. Reliability and advantages

The performance of the framework across 10 trials (Fig. 8) demonstrates strong robustness, with minimal variability in key metrics such as

Table 2
Performance of different machine learning algorithms. The values presented in the table represent the average of evaluation metrics from 10 independent trials. Ranked by performance from best to worst. Meta-Model performs the best, with all metrics higher than others.

No.	Models	Evaluation Metrics			
		R-Pearson	R-squared	RMSE	MAE
1	Meta-Model	0.926	0.832	1.898	1.503
2	NNT	0.873	0.734	2.246	1.799
3	NNFAI	0.87	0.729	2.229	1.808
4	CAT	0.868	0.726	2.425	1.879
5	ERT	0.866	0.723	2.989	2.369
6	LGBM	0.855	0.703	2.307	1.817
7	XGB	0.85	0.694	2.463	1.827
8	RF	0.841	0.678	2.643	2.114
9	KNN	0.730	0.500	2.471	2.051

Notes: The Pearson correlation coefficient (R) and the coefficient of determination (R^2) are primarily used to evaluate how well the model fits the observed data, with values closer to 1 indicating a better fit. The root mean squared error (RMSE) and the mean absolute error (MAE) serve as key metrics for quantifying the discrepancy between predicted and observed values. Notably, RMSE is particularly sensitive to outliers, making it an effective tool for assessing the consistency between predicted and observed values.

R^2, RMSE, and MAE. The standard deviation of R^2 values across trials is approximately 0.0246, indicating that the model consistently performs well and is not sensitive to noise in the data. On the other hand, the generalization ability is evident from its strong performance on the test dataset, which is typically unseen during training. The high R^2 value (0.878) and low RMSE (1.430) and MAE (1.123) in Trial 9 indicate that the model can generalize well to new data.

The meta-model has significantly improved both the accuracy of sand thickness prediction and the rationality of sand distribution. The original sweetness attribute exhibited a limited correlation with sand thickness ($R^2 = 0.169$), whereas the fused attribute of the Meta-Model achieved a substantially higher R^2 value of 0.878 on the test dataset, indicating a much stronger predictive capability (Fig. 10B). Imaging results also show a marked enhancement. The map of the original sweetness attribute displayed vague sand boundaries and discontinuous high-value areas, which obscured the morphological features of channel-bar complexes (Fig. 7A). In contrast, the fused attribute, by integrating seismic attributes from low-, mid-, and high frequency seismic volumes, overcame these limitations. The high-value areas in the map of fused attribute exhibit enhanced continuity and clearer morphology, particularly in the eastern part of the study area, where the shapes of the distributary channel-bar complexes are distinctly outlined (Fig. 8A).

Quantitative validation further confirms the high accuracy of the predictions. The numerical discrepancy between the predicted sand thickness and the real sand thickness from the well logs is minimal (Fig. 8B). On one hand, the individual models selected in the automated machine learning framework have been widely applied and possess strong predictive capabilities in reservoir prediction. On the other hand, the framework employs adaptive multi-algorithm fusion, introducing multi-layer stacking ensembling to mitigate the limitations of individual models (such as the KNN algorithm's sensitivity to data noise). Additionally, repeated k-fold bagging is used for overfitting correction, ultimately achieving a synergistic and complementary integration of different seismic frequency attributes.

The consistent performance across multiple trials, the strong metrics on the test dataset, and the accurate predictions for real-world well data all validate the effectiveness of the automated machine learning framework we have developed. The results provide a robust and reliable new approach for quantitative reservoir characterization in complex sedimentary systems.

6.2. *Application prospects and limitations*

The proposed fusing spectral-decomposed seismic attributes framework based on AutoML exhibits substantial potential for reservoir characterization and hydrocarbon exploration. Spectral decomposition mitigates frequency aliasing, enhancing seismic data clarity. This approach simultaneously mitigates frequency aliasing and decomposes the original seismic data into multiple frequency volumes (e.g., low-, middle-, and high-frequency bands). This results in enhanced data clarity and provides a robust multi-frequency basis for subsequent attributes fusion. Supervised data from well-log interpretation accurately reflects subsurface conditions, improving objectivity and reducing ambiguity from geological variability. The ability to substantially enhance

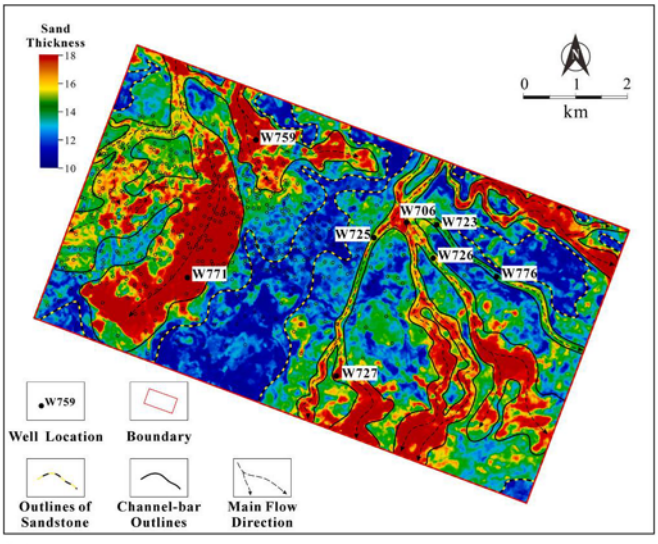

(A)

Fig. 8. The result of fused spectral-decomposed seismic attributes. A) Sandstone thickness predicted by the 9th trial meta-model using multi-frequency (low, middle, and high) Sweetness, RMS amplitude, and Envelope attributes. The result represents the distribution of sandstone, with clear outlines of channel-bar complexes. B) Well profiles from the blind-test dataset, showing wireline logs for GR and SP, illustrating the comparison between log-derived sandstone interpretations and the predicted thickness values.

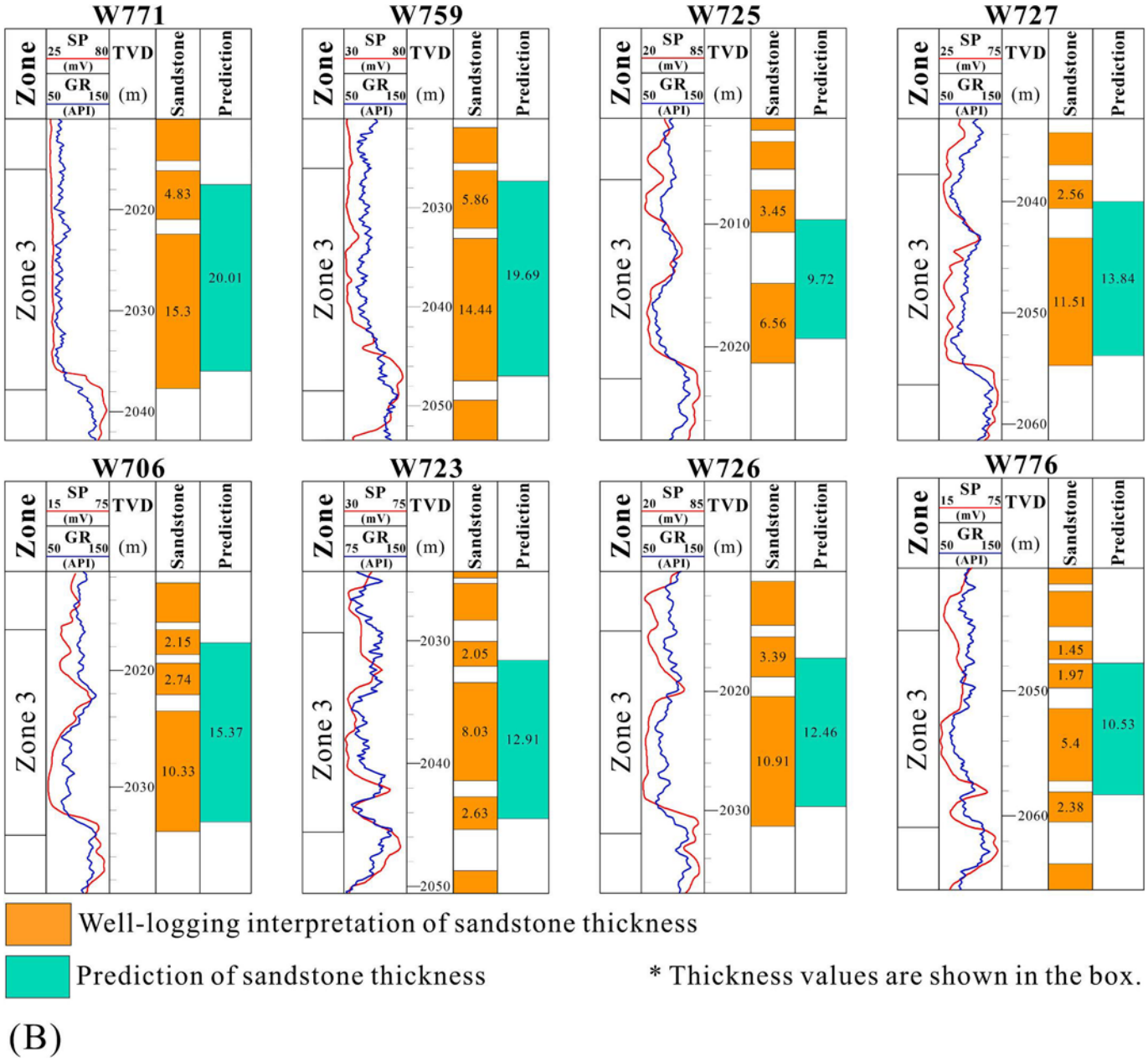

Fig. 8. (*continued*).

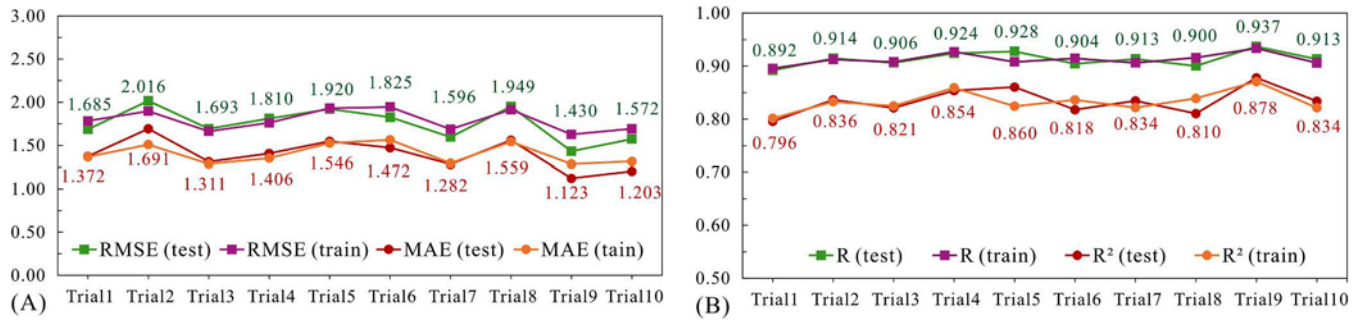

Fig. 9. Performance metrics of the framework across 10 trials. A) The RMSE and MAE of test dataset and train dataset across 10 trials. B) The R and R^2 of test dataset and train dataset across 10 trials. The numbers annotated in the figure are all results from the blind test dataset.

the accuracy of sand thickness prediction and the interpretability of sand body distribution makes it a reliable tool for identifying and delineating sand bodies in complex sedimentary systems. The quantitative reservoir prediction achieved through the fusion of seismic attributes from

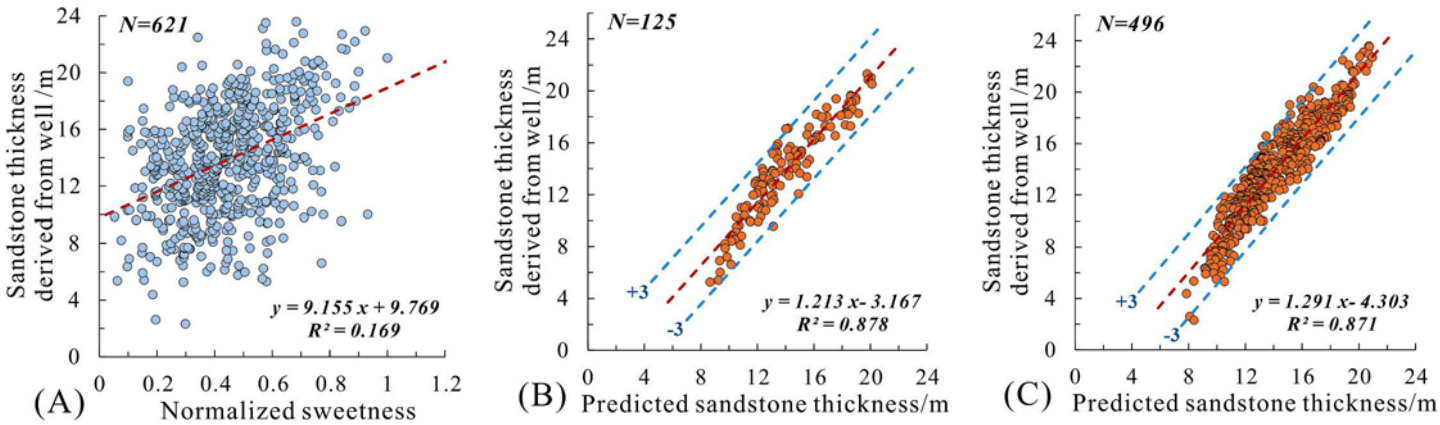

Fig. 10. A) Relationship between the original normalized Sweetness attribute and sandstone thickness derived from wells. (B–C) Relationships between the predicted sandstone thickness and sandstone thickness derived from wells. B) The 125 samples are from the test dataset. C) The 496 samples are from the train dataset.

different frequency bands enables high-resolution prediction of sand thickness distribution, which is crucial for optimizing well placement in complex deltaic depositional systems and reducing drilling risks. Compared to traditional workflows, the framework can significantly reduce the time required for manual interpretation and minimize subjective interference. Additionally, the framework has strong generalization capabilities. The framework is not constrained by lithology and depositional systems, performing various reservoir characterization tasks through by incorporating different datasets. Furthermore, it also provides a practical solution for any supervised learning application.

Despite the numerous advantages demonstrated by AutoML framework for fusing spectral-decomposed seismic attributes we have developed, there is still room for further improvement. The prediction accuracy is constrained by geological heterogeneity and the resolution of the seismic data volume. When the reservoir exhibits strong geological heterogeneity, such as sand bodies mainly occurring as thin beds or interbedded layers, the performance of this method may be compromised. When the quality of the seismic data is poor (e.g. narrow bandwidth or low signal-to-noise ratio), the effectiveness of seismic spectral decomposition will be reduced, thereby leading to unsatisfactory results. Such limitations are commonly acknowledged in seismic attribute analysis. Moreover, the performance of the proposed framework may be potentially influenced by the choice of the spectral decomposition method. In this study, the CWT was adopted primarily due to its wide acceptance and maturity in seismic interpretation, which helps ensure the reproducibility of the workflow and the generalizability of the conclusions. However, the fusion framework itself is independent of the specific spectral decomposition method. Future work could extend the proposed framework by incorporating other advanced spectral decomposition methods to further explore performance improvements.

For larger datasets and more complex geological conditions, the training time of the current automated machine learning framework still has considerable room for optimization. To demonstrate the robustness and generalization of the proposed framework, we adopted a computationally intensive, high-quality strategy. Taking the study area as an example, the seismic data volume covers an area of around 60 km^2, with 621 available well data points. The seismic data volume was divided into three frequency division seismic data volumes, containing nine seismic attributes. Running the framework once on an NVIDIA RTX 4060ti 12G GPU takes nearly three hours. However, for specific reservoir applications, targeted optimizations—such as early stopping to shorten model runtime and pruning underperforming models—can markedly improve training efficiency while preserving predictive accuracy.

7. Conclusions

The results indicated that the proposed method significantly enhanced the accuracy and interpretability of sand thickness prediction in reservoir characterization.

(1) Enhanced sensitivity through fusing spectral-decomposed seismic attributes: Seismic attributes exhibit varying sensitivity to sand thickness. Low-frequency attributes effectively delineate thicker sand bodies, while high-frequency attributes excel in resolving thinner ones. Integrating spectral decomposition attributes markedly improves the resolution of sand thickness predictions.
(2) Significantly improving prediction accuracy and interpretability: The proposed AutoML framework achieved a coefficient of determination (R) of 0.926, with a mean absolute error (MAE) of 1.503. These metrics outperform single machine learning models, demonstrating the ability to provide more reliable and accurate prediction of sand bodies.
(3) Robustness and generalization capability: The robustness and generalization capabilities were validated through multiple trials and independent test datasets. The results showed minimal variability in key metrics such as R^2, RMSE, and MAE across 10 trials, indicating that the model consistently performs well and is not sensitive to noise in the data.
(4) Efficiency in quantitative reservoir characterization: In contrast to conventional workflows, the proposed methodology substantially accelerates interpretation by reducing manual effort and mitigating subjective bias, delivering an efficient and reliable solution for reservoir characterization. Its exceptional adaptability and robustness enable facilitate application across varied depositional systems, lithologies, and petrophysical parameters. This breadth of applicability renders its highly capable of addressing the vast majority of demands in quantitative reservoir characterization.

CRediT authorship contribution statement

Keyu Ren: Writing – original draft, Visualization, Validation, Software, Methodology, Investigation, Formal analysis, Data curation, Conceptualization. **Wei Li:** Writing – review & editing, Supervision, Methodology, Funding acquisition. **Lun Zhao:** Supervision, Resources, Project administration, Data curation. **Wurong Wang:** Supervision, Project administration, Methodology, Investigation. **Jincai Wang:** Resources, Project administration. **Han Wang:** Methodology, Investigation, Data curation. **Yi Li:** Supervision, Project administration, Investigation. **Linbo Qu:** Validation, Software, Methodology. **Dali Yue:** Writing – review & editing, Supervision, Resources, Project administration, Funding acquisition.

Declaration of competing interest

The authors declare that they have no known competing financial interests or personal relationships that could have appeared to influence the work reported in this paper.

Data availability

The authors do not have permission to share data.

References

Abdulaziz, A.M., Mahdi, H.A., Sayyouh, M.H., 2019. Prediction of reservoir quality using well logs and seismic attributes analysis with an artificial neural network: a case study from Farrud Reservoir, Al-Ghani Field, Libya. J. Appl. Geophys. 161, 239–254. https://doi.org/10.1016/j.jappgeo.2018.09.013.

Ali, M., Zhu, P., Jiang, R., Huolin, M., Ehsan, M., Hussain, W., Zhang, H., Ashraf, U., Ullaah, J., 2023. Reservoir characterization through comprehensive modeling of elastic logs prediction in heterogeneous rocks using unsupervised clustering and class-based ensemble machine learning. Appl. Soft Comput. 148, 110843. https://doi.org/10.1016/j.asoc.2023.110843.

Al-Mudhafar, W., 2015. Integrating Bayesian model averaging for uncertainty reduction in permeability modeling. In: Offshore Technology Conference. Presented at the Offshore Technology Conference. OTC, Houston, Texas, USA. https://doi.org/10.4043/25646-MS p. OTC-25646-MS.

Anifowose, F.A., Labadin, J., Abdulraheem, A., 2017. Ensemble machine learning: an untapped modeling paradigm for petroleum reservoir characterization. J. Pet. Sci. Eng. 151, 480–487. https://doi.org/10.1016/j.petrol.2017.01.024.

Bakke, K., Kane, I.A., Martinsen, O.J., Petersen, S.A., Johansen, T.A., Hustoft, S., Jacobsen, F.H., Groth, A., 2013. Seismic modeling in the analysis of deep-water sandstone termination styles. Bulletin 97, 1395–1419. https://doi.org/10.1306/03041312069.

Ballinas, M.R., Bedle, H., Devegowda, D., 2023. Supervised machine learning for discriminating fluid saturation and presence in subsurface reservoirs. J. Appl. Geophys. 217, 105192. https://doi.org/10.1016/j.jappgeo.2023.105192.

Bao, L.-L., Zhang, J.-S., Zhang, C.-X., Guo, R., Wei, X.-L., Jiang, Z.-L., 2023. A reliable Bayesian neural network for the prediction of reservoir thickness with quantified uncertainty. Comput. Geosci. 178, 105409. https://doi.org/10.1016/j.cageo.2023.105409.

Bashir, Y., Akdeniz, D.N., Balci, D., Soner, M., Ozturk, D.U., Tekin, M., Doğan, D., Karaman, A., İmren, C., 2025. 3D geo-seismic data enhancement leveraging geophysical attributes for hydrocarbon prospect and geological illumination. Phys. Chem. Earth Parts A/B/C 138, 103854. https://doi.org/10.1016/j.pce.2025.103854.

Cai, R., Sun, C., Yao, Z., Li, S., 2024. A depth-variant seismic wavelet extraction method for basis pursuit inversion with an impedance trend constraint. GEOPHYSICS 89, R275–R286. https://doi.org/10.1190/geo2023-0255.1.

Cherskiy, N.V., Tsarev, V.P., Nikitin, S.P., 1984. Investigation and Prediction of Conditions of Accumulation of Gas Resources in Gas-Hydrate Pools (Northeast USSR and Kamchatka), 21, pp. 84–89.

Chopra, S., Marfurt, K.J., 2005. Seismic attributes — a historical perspective. Geophysics 70, 3SO–28SO. https://doi.org/10.1190/1.2098670.

Erickson, N., Mueller, J., Shirkov, A., Zhang, H., Larroy, P., Li, M., Smola, A., 2020. Autogluon-tabular: robust and accurate AutoML for structured data. https://doi.org/10.48550/arXiv.2003.06505.

Guo, H., Lewis, S., Marfurt, K.J., 2008. Mapping multiple attributes to three- and four-component color models — a tutorial. GEOPHYSICS 73, W7–W19. https://doi.org/10.1190/1.2903819.

Haiyang, Y., Tongjun, C., xiong, S., Haicheng, X., Wan, L., 2023. Methods for predicting the thickness of coal seams based on seismic attribute optimization and machine learning. Coal Geol. Explor. 51, 164–170.

Halder, R.K., Uddin, M.N., Uddin, Md.A., Aryal, S., Khraisat, A., 2024. Enhancing K-nearest neighbor algorithm: a comprehensive review and performance analysis of modifications. J. Big Data 11, 113. https://doi.org/10.1186/s40537-024-00973-y.

Hampson, D.P., Schuelke, J.S., Quirein, J.A., 2001. Use of multiattribute transforms to predict log properties from seismic data. GEOPHYSICS 66, 220–236. https://doi.org/10.1190/1.1444899.

Hart, B.S., 2008. Channel Detection in 3-D Seismic Data using Sweetness. AAPG Bull. 92, 733–742. https://doi.org/10.1306/02050807127.

He, X., Zhao, K., Chu, X., 2021. AutoML: a survey of the state-of-the-art. Knowl.-Based Syst. 212, 106622. https://doi.org/10.1016/j.knosys.2020.106622.

Hosseinyar, G., Moussavi-Harami, R., Abdollahie Fard, I., Mahboubi, A., Noemani Rad, R., 2019. Seismic geomorphology and stratigraphic trap analyses of the lower cretaceous siliciclastic reservoir in the Kopeh Dagh-Amu Darya Basin. Pet. Sci. 16, 776–793. https://doi.org/10.1007/s12182-019-0347-1.

Iturrarán-Viveros, U., Parra, J.O., 2014. Artificial Neural Networks applied to estimate permeability, porosity and intrinsic attenuation using seismic attributes and well-log data. J. Appl. Geophys. 107, 45–54. https://doi.org/10.1016/j.jappgeo.2014.05.010.

Jia, W., Zong, Z., Qin, D., Lan, T., 2023. A method for predicting the TOC in source rocks using a machine learning-based joint analysis of seismic multi-attributes. J. Appl. Geophys. 216, 105143. https://doi.org/10.1016/j.jappgeo.2023.105143.

Kiritchkova, A.I., Nosova, N.V., 2014. The Lower Jurassic of the Eastern Caspian region and the Middle Caspian Basin: Lithology, facies, taphonomy. Stratigr. Geol. Correl. 22, 479–493. https://doi.org/10.1134/S0869593814050050.

Koson, S., Chenrai, P., Choowong, M., 2014. Seismic Attributes and their applications in Seismic Geomorphology, 6. BEST.

Kozhagulova, A., Dillinger, A., Bayramov, E., Iltukov, R., Holbrook, J., Fustic, M., 2023. Geothermal energy potential of the Mangyshlak Basin, western Kazakhstan: a preliminary assessment based on stratigraphy and temperature data. Geothermics 109, 102655. https://doi.org/10.1016/j.geothermics.2023.102655.

Krause, P., Boyle, D.P., Bäse, F., 2005. Comparison of different efficiency criteria for hydrological model assessment. In: Advances in Geosciences. Presented at the Proceedings of the 8th Workshop for Large Scale Hydrological Modelling - Oppurg 2004 - 8th workshop for Large-scale hydrological modelling, Oppurg, Germany, 11–13 November 2004. Copernicus GmbH, pp. 89–97. https://doi.org/10.5194/adgeo-5-89-2005.

Li, W., Yue, D., Wang, Wenfeng, Wang, Wurong, Wu, S., Li, J., Chen, D., 2019. Fusing multiple frequency-decomposed seismic attributes with machine learning for thickness prediction and sedimentary facies interpretation in fluvial reservoirs. J. Pet. Sci. Eng. 177, 1087–1102. https://doi.org/10.1016/j.petrol.2019.03.017.

Li, W., Yue, D., Wu, S., Shu, Q., Wang, W., Long, T., Zhang, B., 2020. Thickness prediction for high-resolution stratigraphic interpretation by fusing seismic attributes of target and neighboring zones with an SVR algorithm. Mar. Pet. Geol. 113, 104153. https://doi.org/10.1016/j.marpetgeo.2019.104153.

Li, W., Yue, D., Colombera, L., Duan, D., Long, T., Wu, S., Liu, Y., 2023. A novel method for seismic-attribute optimization driven by forward modeling and machine learning in prediction of fluvial reservoirs. Geoenergy Sci. Eng. 227, 211952. https://doi.org/10.1016/j.geoen.2023.211952.

Li, H.-H., Yue, D.-L., Li, W., Dan, L.-L., Liu, Y., Wang, W.-R., Ren, K.-Y., Tan, L., 2025. Sedimentary architecture characterization by combining well logs and seismic data in river-dominated delta reservoirs: the Pearl River Mouth Basin, South China Sea. J. Palaeogeogr. 14, 100249. https://doi.org/10.1016/j.jop.2025.03.004.

Lin, L., Zhong, Z., Li, C., Gorman, A., Wei, H., Kuang, Y., Wen, S., Cai, Z., Hao, F., 2024. Machine learning for subsurface geological feature identification from seismic data: methods, datasets, challenges, and opportunities. Earth Sci. Rev. 257, 104887. https://doi.org/10.1016/j.earscirev.2024.104887.

Liu, H., Xia, Q.-L., Zhou, X.-H., 2018. Geologic-seismic models, prediction of shallow-water lacustrine delta sandbody and hydrocarbon potential in the Late Miocene, Huanghekou Sag, Bohai Bay Basin, northern China. J. Palaeogeogr. 7, 66–87. https://doi.org/10.1016/j.jop.2017.11.001.

Liu, L., Li, W., Du, Y., Yue, D., Zhang, X., Hou, J., 2024. Reservoir prediction method of fusing frequency-decomposed seismic attributes using Stacking ensemble learning. Oil Geophys. Prospect. 59, 12–22. https://doi.org/10.13810/j.cnki.issn.1000-7210.2024.01.002.

McArdle, N.J., Ackers, M.A., 2012. Understanding seismic thin-bed responses using frequency decomposition and RGB blending. First Break 30. https://doi.org/10.3997/1365-2397.2012022.

Na'imi, S.R., Shadizadeh, S.R., Riahi, M.A., Mirzakhanian, M., 2014. Estimation of reservoir porosity and water saturation based on seismic attributes using support Vector Regression Approach. J. Appl. Geophys. 107, 93–101. https://doi.org/10.1016/j.jappgeo.2014.05.011.

Nash, J.E., Sutcliffe, J.V., 1970. River flow forecasting through conceptual models part I — a discussion of principles. J. Hydrol. 10, 282–290. https://doi.org/10.1016/0022-1694(70)90255-6.

Ni, J., Zhao, D., Liao, X., Li, X., Fu, L., Chen, R., Xia, Z., Liu, Y., 2022. Sedimentary architecture analysis of deltaic sand bodies using sequence stratigraphy and seismic sedimentology: a case study of Jurassic Deposits in Zhetybay Oilfield, Mangeshrak Basin, Kazakhstan. Energies 15, 5306. https://doi.org/10.3390/en15145306.

Pang, X.-J., Wang, G.-M., Zhao, M., Wang, Q.-B., Zhang, X.-F., 2024. The reservoir characteristics and their controlling factors of the sublacustrine fan in the Paleogene Dongying Formation, Bohai Sea, China. J. Palaeogeogr. 13, 127–148. https://doi.org/10.1016/j.jop.2023.10.002.

Posamentier, H.W., Paumard, V., Lang, S.C., 2022. Principles of seismic stratigraphy and seismic geomorphology I: Extracting geologic insights from seismic data. Earth Sci. Rev. 228, 103963. https://doi.org/10.1016/j.earscirev.2022.103963.

Quaranta, L., Azevedo, K., Calefato, F., Kalinowski, M., 2025. A multivocal literature review on the benefits and limitations of industry-leading AutoML tools. Inf. Softw. Technol. 178, 107608. https://doi.org/10.1016/j.infsof.2024.107608.

Salehin, I., Islam, Md.S., Saha, P., Noman, S.M., Tuni, A., Hasan, Md.M., Baten, Md.A., 2024. AutoML: a systematic review on automated machine learning with neural architecture search. J. Informa. Intel. 2, 52–81. https://doi.org/10.1016/j.jiixd.2023.10.002.

Shahsenov, I., Malikov, R., Cook, P., Grant, S., Ismayilov, N., Abbasov, K., 2022. Prediction of Gamma Ray data from pre-stack seismic reflection partial angle stacks using Continuous Wavelet Transform and convolutional neural network approach. J. Appl. Geophys. 197, 104523. https://doi.org/10.1016/j.jappgeo.2021.104523.

Shen, Z., Zhang, Y., Wei, L., Zhao, H., Yao, Q., 2018. Automated machine learning: from principles to practices. https://doi.org/10.48550/ARXIV.1810.13306.

Sinha, S., Routh, P.S., Anno, P.D., Castagna, J.P., 2005. Spectral decomposition of seismic data with continuous-wavelet transform. Geophysics 70, P19–P25. https://doi.org/10.1190/1.2127113.

Tian, G., Lin, N., Zhang, K., Yang, J., Zhang, C., 2021. Prediction of seismic oil and gas reservoir using self-organizing neural network from multi-component seismic data. Sci. Technol. Eng. 21, 7931–7941.

Torrence, C., Compo, G.P., 1998. A practical guide to wavelet analysis. Bull. Amer. Meteor. Soc. 79, 61–78. https://doi.org/10.1175/1520-0477(1998)079<0061:APGTWA>2.0.CO;2.

Widess, M.B., 1973. How thin is a thin bed? Geophysics 38, 1176–1180. https://doi.org/10.1190/1.1440403.

Xu, Z.-H., Wu, S.-H., Plink-Björklund, P., Zhang, T., Yue, D.-L., Qian, Q.-H., Li, Q., Feng, W.-J., 2025. Autocyclic switching processes and architecture of lobes in river-dominated lacustrine deltas. J. Palaeogeogr. 14, 126–140. https://doi.org/10.1016/j.jop.2024.12.004.

Xue, Y., Cao, J., Tian, R., Du, H., Shu, Y., 2014. Application of the empirical mode decomposition and wavelet transform to seismic reflection frequency attenuation analysis. J. Pet. Sci. Eng. 122, 360–370. https://doi.org/10.1016/j.petrol.2014.07.031.

Yao, Y., Sun, D., Xu, J.-H., Wang, B., Peng, G., Sun, B., 2023. Evaluation of enhanced oil recovery methods for mature continental heavy oil fields in China based on geology, technology and sustainability criteria. Energy 278, 127962. https://doi.org/10.1016/j.energy.2023.127962.

Yue, D., Li, W., Wang, W., Sun, P., Wu, S., Xu, Z., Liu, L., Wu, D., Qu, L., Ren, K., Lin, J., Zhang, S., 2025. Advances and perspectives in intelligent characterization and modeling of clastic reservoirs. J. Palaeogeogr. (Chinese Edition) 27, 903–923.

Yue, D., Li, W., Wang, Wurong, Hu, G., Qiao, H., Hu, J., Zhang, M., Wang, Wenfeng, 2019. Fused spectral-decomposition seismic attributes and forward seismic modelling to predict sand bodies in meandering fluvial reservoirs. Mar. Pet. Geol. 99, 27–44. https://doi.org/10.1016/j.marpetgeo.2018.09.031.

Yue, D., Li, W., Du, Y., Hu, G., Wang, W., Wang, Wurong, Wang, Z., Xian, Benzhong, 2022. Review on optimization and fusion of seismic attributes for fluvial reservoir characterization. Earth Sci. 47, 3929–3943.

Zeng, H., 2017. Thickness imaging for high-resolution stratigraphic interpretation by linear combination and color blending of multiple-frequency panels. Interpretation 5, T411–T422. https://doi.org/10.1190/INT-2017-0034.1.

Zeng, H., Backus, M.M., 2005. Interpretive advantages of 90°-phase wavelets: part 1 — modeling. Geophysics 70, C7–C15. https://doi.org/10.1190/1.1925740.

Zeng, H., Ambrose, W.A., Villalta, E., 2001. Seismic sedimentology and regional depositional systems in Mioceno Norte, Lake Maracaibo, Venezuela. Lead. Edge 20, 1260–1269. https://doi.org/10.1190/1.1487259.

Zhang, B., Liu, Y., Pelissier, M., Hemstra, N., 2014. Semiautomated fault interpretation based on seismic attributes. Interpretation 2, SA11–SA19. https://doi.org/10.1190/INT-2013-0060.1.

Zhang, J., Shan, X., Huo, S., Huang, L., Zheng, W., Zhou, X., Liu, E., 2025. Deep learning-driven multi-frequency seismic inversion for enhanced thin-layer stratigraphic characterization. J. Appl. Geophys. 239, 105749. https://doi.org/10.1016/j.jappgeo.2025.105749.

Zöller, M.-A., Huber, M.F., 2021. Benchmark and Survey of Automated Machine Learning Frameworks. https://doi.org/10.48550/arXiv.1904.12054.